

Ultra-compact structure in radio quasars as a cosmological probe: a revised study of the interaction between cosmic dark sectors

Xiaogang Zheng^{1,2}, Marek Biesiada^{1,2}, Shuo Cao^{1*}, Jingzhao Qi¹, and Zong-Hong Zhu¹

¹ *Department of Astronomy, Beijing Normal University, Beijing 100875, China;
caoshuo@bnu.edu.cn*

² *Department of Astrophysics and Cosmology, Institute of Physics, University of Silesia,
Uniwersytecka 4, 40-007 Katowice, Poland*

ABSTRACT

A new compilation of 120 angular-size/redshift data for compact radio quasars from very-long-baseline interferometry (VLBI) surveys motivates us to revisit the interaction between dark energy and dark matter with these probes reaching high redshifts $z \sim 3.0$. In this paper, we investigate observational constraints on different phenomenological interacting dark energy (IDE) models with the intermediate-luminosity radio quasars acting as individual standard rulers, combined with the newest BAO and CMB observation from *Planck* results acting as statistical rulers. The results obtained from the MCMC method and other statistical methods including Figure of Merit and Information Criteria show that: (1) Compared with the current standard candle data and standard clock data, the intermediate-luminosity radio quasar standard rulers, probing much higher redshifts, could provide comparable constraints on different IDE scenarios. (2) The interaction between dark energy and dark matter seems to be vanishing or slightly smaller than zero. At the 68.3% confidence level, the energy is seen transferred from dark matter to dark energy, which implies that those IDE models can not alleviate the coincidence problem or even more sever. However, the strong degeneracies between the interaction term and Hubble constant may contribute to alleviate the tension of H_0 between the recent *Planck* and *HST* measurements. (3) Concerning the ranking of competing dark energy models, IDE with more free parameters are substantially penalized by the BIC criterion, which agrees very well with the previous results derived from other cosmological probes.

Subject headings: expansion history – cosmology: observations – methods: statistical

1. Introduction

Dark energy has become one of the most important issues of modern cosmology since many astrophysical and cosmological observations such as Type Ia Supernovae (SN Ia) (Riess et al. 1998; Perlmutter et al. 1999), Large Scale Structure (LSS) (Eisenstein et al. 2005) and cosmic microwave

background radiation (CMB) (Komatsu et al. 2011) coherently indicate that the universe is undergoing an accelerated expansion at the present stage. The most simple candidate for the uniformly distributed material component responsible for this behaviour, is some form of vacuum energy density or cosmological constant Λ . Despite its simplicity, the simple cosmological constant is always entangled with the well-known coincidence problem: the matter density ρ_m decreases with the expansion of the universe as a^{-3} and the density of cosmological constant ρ_Λ does not change with the expansion of the universe, whereas the matter density is comparable with the dark energy density today. More recent works have implied that this simple Λ CDM model encounters other problems. For instance, a tension between Λ CDM and the measurements of Hubble parameter ($H(z)$) has been extensively discussed in the framework of different Om diagnostics (Sahni et al. 2014; Ding et al. 2015; Zheng et al. 2016). Moreover, the local measurement of Hubble constant (H_0) through the Wide Field Camera 3 (WFC3) on the Hubble Space Telescope (*HST*) (Riess et al. 2016) suggests a higher value of H_0 than the prediction of Λ CDM model from *Planck* CMB data (Planck Collaboration XIII 2016). In order to meet these problems, the consideration of the possibility of exchanging energy between DE and DM through an interaction term seems feasible, as the coupling between these dark sectors can provide a mechanism to alleviate the coincidence problem (Amendola 2000; Olivares et al. 2006; Wang et al. 2016) and provide possible a larger value of H_0 derived from the recent *HST* measurement.

However, the nature of DE and DM remains a mystery and most of the investigation of interaction is based on the phenomenological assumptions. As extensively considered in the literature (see e.g. Dalal et al. (2001); Guo et al. (2007); Li et al. (2016)), we assume that dark energy and dark matter exchange energy through an interaction term Q , while there is no interaction between baryonic matter and dark energy

$$\begin{aligned}\dot{\rho}_X + 3H(\rho_X + p_X) &= -Q, \\ \dot{\rho}_c + 3H\rho_c &= Q, \\ \dot{\rho}_b + 3H\rho_b &= 0.\end{aligned}\tag{1}$$

where ρ_X , ρ_c and ρ_b denote the energy density of dark energy, cold dark matter and baryonic matter, respectively. In fact, in the standard model of particle physics combined with the solar system experiments (Will 2001), the coupling between dark energy and baryons is basically constrained to irrelevantly small values. This is in agreement with the results obtained in the modified interacting dark energy (MIDE) model as a candidate to describe possible interaction between dark energy and dark matter as well as that between dark energy and baryonic matter (Cao et al. 2015).

Note that with the ansatz (1), the total energy density is conserved: $\dot{\rho}_{tot} + 3H(\rho_{tot} + p_{tot}) = 0$. If Q is a non-zero function of the scale factor, the interaction makes ρ_m and ρ_X to deviate from the standard scaling. Considering from continuity equations, the interaction term Q must be a function multiplied by the energy density and a quantity said the inverse of time which can be considered by the Hubble factor H . The simplest assumptions including a freedom of choice concerning the form of the energy density are $Q = Q(H\rho_c)$ and $Q = Q(H\rho_X)$ (see Cao et al. (2013) and references

therein). We assume that, for the phenomenological interaction models, the equation of state (EoS) of dark energy $w_X \equiv p/\rho$ is constant in spatially flat FRW metric. The standard cosmology without interaction between dark energy and dark matter is recovered with $Q = 0$, while $Q \neq 0$ denotes non-standard cosmology. On the other hand, the value of Q determines the extent of interaction and transfer direction between dark energy and dark matter, i.e., $Q < 0$ indicates that the energy is transferred from dark matter to dark energy, while $Q > 0$ denotes that the energy is transferred from dark energy to dark matter.

In the previous works, different interacting dark energy models have been discussed with various cosmological observations (Feng et al. 2008; Cao et al. 2011; Pan et al. 2012; Cao et al. 2013; Xia et al. 2016; Costa et al. 2017). Recently, the angular size of compact structure in radio quasars versus redshift data from the very-long-baseline interferometry (VLBI) observations have become an effective probe in cosmology and astrophysics (Cao et al. 2017a,b). Based on a 2.29 GHz VLBI all-sky survey of 613 milliarcsecond ultra-compact radio sources, Cao et al. (2017b) extracted a sub-sample of 120 intermediate-luminosity quasars in the redshift range of $0.46 < z < 2.8$, which can be used as cosmological standard rulers with the linear sizes calibrated by a cosmological-model-independent method. Compared with the commonly-used SN Ia standard candles ($z \sim 1.4$), the advantage of this data set is that quasars are observed at much higher redshifts ($z \sim 3.0$), which motivates us to investigate the possible interaction between dark energy and dark matter at higher redshifts. To reduce the uncertainty and put tighter constraint on the value of the coupling, we add, in our discussion, the CMB observation from the *Planck* results as well as the BAO measurements both from the low- z Galaxy and higher- z Lyman- α Forests (Ly α F) data. We expect that sensitivities of measurements of different observables can give complementary results on the coupling between dark sectors.

This paper is organized as follows: The Friedmann equations in the IDE models are presented in Section 2. In Section 3, we introduce the observational data including QSO, BAO and CMB and the corresponding methodology. In Section 4, we perform a Markov Chain Monte Carlo (MCMC) analysis, and furthermore apply the Figure of Merit (FoM) and two model selection techniques, i.e., the Akaike Criterion (AIC) and Bayesian Information Criterion (BIC). Finally the results are summarized in Section 5.

2. The interacting dark energy models

In this paper, in order to derive stringent constraints on the interaction between DE and DM, having in mind the well known degeneracy between model parameters, we assume a flat universe which is strongly supported by CMB data. In a zero-curvature universe filled with ordinary pressureless dust matter (cold dark matter plus baryons), radiation and dark energy, the Friedmann equation reads

$$\rho = \rho_b + \rho_c + \rho_X + \rho_r = 3H^2(z)/8\pi G \quad (2)$$

where ρ_r is the energy density of radiation. We remark here that the effect of this radiation term, which is negligible for low- z observations, should be taken into account when considering the redshifts at photo-decoupling epoch z_* and baryon-drag epoch z_d for the comoving sound horizon in CMB and BAO. Obviously, the dimensionless expansion rate of the Universe, $E(z)$, without the interaction between dark matter and dark energy can be expressed as

$$E^2(z; \mathbf{p}) = (\Omega_{b0} + \Omega_{c0})(1+z)^3 + \Omega_{r0}(1+z)^4 + \Omega_X(z). \quad (3)$$

where $\Omega_{b0} = (8\pi G\rho_{b0})/(3H_0^2)$ is the current baryonic matter component, $\Omega_{c0} = (8\pi G\rho_{c0})/(3H_0^2)$ is the current dark matter component, the current radiation component $\Omega_{r0} = (8\pi G\rho_{r0})/(3H_0^2) = 4.1736 \times 10^{-5}h^{-2}$ (Komatsu et al. 2009), and the dark energy component

$$\Omega_X(z) = (1 - \Omega_{b0} - \Omega_{c0} - \Omega_{r0}) \times (1+z)^{3(1+w)}. \quad (4)$$

In our analysis, we assume that dark energy and cold dark matter exchange energy through interaction term Q proportional to different energy densities ρ_i , i.e., $Q = 3\gamma_i H \rho_i$, where γ_i is a dimensionless constant. The simplest assumption with the freedom to choose the form of the energy density are

$$Q_1 = 3\gamma_c H \rho_c \quad (5)$$

and

$$Q_2 = 3\gamma_d H \rho_X, \quad (6)$$

where the constants γ_c and γ_d quantify the extent of interaction between cold dark matter and dark energy. Correspondingly, $\gamma_i = 0$ indicates that there is no interaction between dark energy and dark matter, while the energy is transferred from dark matter to dark energy when $\gamma_i < 0$, and from dark energy to dark matter when $\gamma_i > 0$. For the first case, the interaction term Q is proportional to the energy density of cold dark matter ρ_c . Combining Eq.(1) and the corresponding expression of Eq.(5), we obtain the energy density of dark matter and dark energy as $\rho_c = \rho_{c0}(1+z)^{3(1-\gamma_c)}$ and $\rho_X = C(1+z)^{3(1+w)} - \frac{\gamma_c \rho_{c0}}{\gamma_c + w}(1+z)^{3(1-\gamma_c)}$, where C is an integral constant to be determined. From the Friedmann equation ($H^2(z) = 8\pi G(\rho_b + \rho_c + \rho_X + \rho_r)/3$) combined with $H_0^2 = 8\pi G\rho_{cr}/3$, the Hubble parameter for this interacting dark energy model (which is denoted as γ_c IWCDM model hereafter) is written as

$$\begin{aligned} E^2(z) &= \frac{w\Omega_{c0}}{\gamma_c + w}(1+z)^{3(1-\gamma_c)} + \Omega_{b0}(1+z)^3 + \Omega_{r0}(1+z)^4 \\ &+ (1 - \Omega_{b0} - \Omega_{r0} - \frac{w\Omega_{c0}}{\gamma_c + w})(1+z)^{3(1+w)}. \end{aligned} \quad (7)$$

It can be seen that vanishing interaction term $\gamma_c = 0$, corresponds to the well-known WCDM parametrization. Moreover, in our analysis we will consider another special case of the γ_c IWCDM model with $w = -1$, i.e., the possibility that the cosmological constant (vacuum energy) exchange energy with dark matter through an interaction term γ_c , which is denoted as γ_c IACDM model hereafter. For the second case, when the interaction is proportional to the dark energy density ρ_X

(which is denoted as γ_d IWCDM model hereafter), the dimensionless expansion rate of the Universe reads

$$E^2(z) = \frac{w(\Omega_{b0} + \Omega_{c0}) + \gamma_d}{w + \gamma_d}(1+z)^3 + \Omega_{r0}(1+z)^4 + \frac{w(1 - \Omega_{b0} - \Omega_{c0})}{w + \gamma_d}(1+z)^{3(1+w+\gamma_d)}. \quad (8)$$

which corresponds to the γ_d I Λ CDM model with $w = -1$.

Let us emphasize the use of the Hubble constant H_0 in our analysis. Considering the tension of its precise value between different astrophysical methods, i.e., Cepheids from the Hubble Space Telescope (*HST*) key project (Riess et al. 2016) and CMB data from the *Planck* satellite experiment (Planck Collaboration XIV 2016), we will keep the Hubble constant as a free parameter, which will be constrained by the observational data described below. Therefore, the interacting dark energy models considered in this paper have five parameters (Ω_{b0} , Ω_{c0} , w , γ_i and H_0), where Ω_{b0} and Ω_{c0} specify the current density of baryonic matter and dark matter, w denotes the equation of state of dark energy, γ_c and γ_d presents how strongly dark energy interacts with dark matter.

3. Observational data and methodology

In this work, we will consider a combination of three types of standard rulers to derive the information of angular diameter distances and thus the interaction between dark sectors at different redshifts, i.e., the compact radio quasars data from VLBI, the cosmic microwave background (CMB) measurements from the *Planck* results, and the baryonic acoustic oscillations (BAO) from the low- z galaxy data and the higher- z Lyman- α Forests(Ly α F) data. The first probes can be considered as individual standard rulers while the other two probes are treated as statistical standard rulers in cosmology.

3.1. Individual standard rulers: QSO

It is well known that for objects with determined intrinsic physical size, one can determine the corresponding angular diameter distances by measuring their angular sizes at different redshifts. As is extensively discussed in the literature (Gurvits 1994), the linear sizes of compact structure in radio sources could depend on the luminosity and redshift as

$$l_m = lL^\beta(1+z)^n \quad (9)$$

where β and n are the two parameters respectively characterizing the “angular size - luminosity” and “angular size - redshift” relations. However, the most recent analysis (Cao et al. 2017a) indicated that only a sub-sample of intermediate-luminosity radio quasars (10^{27} W/Hz $< L < 10^{28}$

W/Hz) could serve as a standard cosmological rod, whose linear sizes shows negligible dependent on luminosity and redshift ($\beta \simeq 10^{-4}$, $|n| \simeq 10^{-3}$). Let us stress that sample selection in terms of luminosity, which involves the knowledge of angular diameter distances to the quasars, can be performed in a robust way not depending on the details of cosmological model (for details see (Cao et al. 2017a)) and does not induce circularity problems in using QSOs for cosmological model parameter inference. For the observational quasar data, we adopt the measurements of 120 intermediate-luminosity radio quasars in the redshift range $0.46 < z < 2.80$, the linear size of which is calibrated to $l_m = 11.03 \pm 0.25$ pc by a new cosmology-independent technique using cosmic chronometer (Cao et al. 2017b).

The angular size of the compact structure in intermediate-luminosity radio quasars, observed at redshifts z , can be theoretically expressed as

$$\theta_{th}(z) = \frac{l_m}{D_A(z)} \quad (10)$$

where D_A is the angular diameter distance computed in the models of interest, which reads

$$D_A(z; \mathbf{p}) = \frac{c}{H_0} \frac{1}{1+z} \int_0^z \frac{dz'}{E(z'; \mathbf{p})} \quad (11)$$

in flat Friedman-Robertson-Walker metric. In order to constrain the model parameters \mathbf{p} using these quasar data, we define the likelihood function $\mathcal{L}_{QSO} \propto \exp[-\chi_{QSO}^2(z; \mathbf{p})/2]$, where χ_{QSO}^2 is related to the quasar sample as

$$\chi_{QSO}^2 = \sum_{i=1}^{120} \frac{[\theta_{obs}(z_i) - \theta_{th}(z_i; \mathbf{p})]^2}{\sigma_\theta^2(z_i)}. \quad (12)$$

In the above expression, θ_{obs} is the angular size of the compact structure from observations and $\sigma_\theta(z_i)$ is the corresponding total uncertainty (both statistical and systematical uncertainty) for the i th quasar.

3.2. Statistical standard rulers: CMB and BAO

The first statistical standard ruler used in our analysis is the cosmic microwave background (CMB), providing the sound horizon scale at high redshift ($z \sim 1089$), useful for determining the properties of dark sectors in the Universe. For the CMB data, we will use the measurements of several quantities derived from *Planck* (Planck Collaboration XIV 2016), which include the acoustic scale (l_A), the shift parameter (R), and the baryonic matter fraction at the redshift of recombination ($\Omega_{b0}h^2$). Firstly, the acoustic scale is expressed as

$$l_A \equiv (1 + z_*) \frac{\pi D_A(z_*)}{r_s(z_*)} \quad (13)$$

where the redshift of photon-decoupling period can be calculated as (Hu & Sugiyama 1996)

$$z_* = 1048[1 + 0.00124(\Omega_{b0}h^2)^{-0.738}][1 + g_1(\Omega_{m0}h^2)^{g_2}] \quad (14)$$

$$g_1 = \frac{0.0783(\Omega_{b0}h^2)^{-0.238}}{1 + 39.5(\Omega_{b0}h^2)^{0.763}}, g_2 = \frac{0.560}{1 + 21.1(\Omega_{b0}h^2)^{1.81}} \quad (15)$$

The comoving sound horizon can be parameterized as

$$\begin{aligned} r_s(z_*) &= \int_0^t \frac{c_s dt'}{a} = \frac{c}{H_0} \int_{z_*}^{\infty} \frac{c_s dz}{E(z)} \\ &= \frac{c}{H_0} \int_0^{a_*} \frac{da}{a^2 E(a) \sqrt{3(1 + \overline{R}_b a)}}. \end{aligned} \quad (16)$$

with $\overline{R}_b = 31500(T_{CMB}/2.7K)^{-4}\Omega_{b0}h^2$ and $T_{CMB} = 2.7255K$. Note that the current radiation component is related to the matter density as $\Omega_{r0} = \Omega_{m0}/(1 + z_{eq})$, where $z_{eq} = 2.5 \times 10^4 \Omega_{m0} h^2 (T_{CMB}/2.7K)^{-4}$. Secondly, the other commonly-used CMB shift parameter reads (Bond et al. 1997)

$$R(z_*) \equiv \frac{(1 + z_*)D_A(z_*)\sqrt{\Omega_{m0}H_0^2}}{c} \quad (17)$$

Model parameters can be estimated from the CMB data using the likelihood based on the χ^2 function defined as

$$\chi_{CMB}^2 = \Delta P_{CMB}^T C_{CMB}^{-1} \Delta P_{CMB} \quad (18)$$

where ΔP_{CMB} is the difference between the theoretical distance priors and the observational counterparts. The corresponding inverse covariance matrix C_{CMB}^{-1} can be found in Table. 4 provided by Planck Collaboration XIV (2016).

The second statistical standard ruler applied in our analysis is the baryonic acoustic oscillations (BAO) scale, the measurements of which are derived from both the low- z galaxy and higher- z Lyman- α Forests(Ly α F) data. For the lower-redshift BAO observations, we turn to the latest measurements of acoustic-scale distance ratio from the 6-degree Field Galaxy Survey (6dFGS) (Beutler et al. 2011), the 'main galaxy sample' from Sloan Digital Sky Survey (SDSS-MGS) (Ross et al. 2015), and the two principal Baryon Oscillation Spectroscopic Survey (BOSS) galaxy samples (BOSS-LOWZ and BOSS-CMASS) (Anderson et al. 2014), while for the the higher- z measurement is derived from SDSS DR12 (Bautista et al. 2017). Now three different types of distance ratios $D_V(z)/r_s(z_d)$, $D_M(z)/r_s(z_d)$ and $D_H(z)/r_s(z_d)$ are listed in Table. 1. We remark that $r_s(z_d)$ is the comoving sound horizon at the baryon-drag epoch z_d (Eisenstein & Hu 1998)

$$z_d = \frac{1291(\Omega_{m0}h^2)^{0.251}}{1 + 0.659(\Omega_{m0}h^2)^{0.828}} [1 + b_1(\Omega_{b0}h^2)^{b_2}] \quad (19)$$

with

$$\begin{aligned} b_1 &= 0.313(\Omega_{m0}h^2)^{-0.419} [1 + 0.607(\Omega_{m0}h^2)^{0.674}], \\ b_2 &= 0.238(\Omega_{m0}h^2)^{0.223}. \end{aligned} \quad (20)$$

$D_V(z)$, $D_M(z)$ and $D_H(z)$ represent the volume-averaged effective distance ($[(1+z)^2 D_A^2(z) cz/H(z)]^{1/3}$), the comoving angular-diameter distance ($(1+z)D_A(z)$), and the Hubble distance ($c/H(z)$), respectively. The χ^2 function constructed from the BAO observations is denoted as χ_{BAO}^2 hereafter.

We will present a combined analysis of the above mentioned three probes used to fit theoretical models to observational data, i.e., the best-fitted parameters of the interacting dark energy models obtained by minimizing $\chi_{ADD}^2 = \chi_{QSO}^2 + \chi_{CMB}^2 + \chi_{BAO}^2$. In adopting the MCMC approach, we generate a chain of sample points distributed in the parameter space according to the posterior probability by using the Metropolis-Hastings algorithm with uniform prior probability distribution, and then repeat this process until the established convergence accuracy can be satisfied. Our code is based on CosmoMC (Lewis & Bridle 2002) and we generated eight chains after setting $R-1 = 0.001$ to guarantee the accuracy of the fits.

4. Results and discussion

In order to demonstrate the constraining power of quasars on the interaction between DE and DM, fitting results from the compact structure measurements of 120 quasars are shown in Fig. 1, in the framework of the γ_c IWCDM and γ_d IWCDM models. As it is well known, the evidence for cosmic acceleration came from other type of standard probes in cosmology, i.e., type Ia supernovae (SN Ia) probing the luminosity distance (D_L) and the age of passively evolving early-type galaxies (cosmic chronometers) providing the direct measurements of Hubble parameter ($H(z)$). In order to compare the QSO fits with the results obtained using SN Ia and $H(z)$, likelihood contours obtained with the latest Union2.1 compilation (Suzuki et al. 2012) consisting of 580 SN Ia in the redshift range $0.014 < z < 1.415$ and 30 Hubble parameter measurements (Zheng et al. 2016) in the redshift range $0.07 < z < 1.965$ are also added for comparison. It is clear that the quasar data could provide constraints comparable to the other two types of standard probes, i.e., the standard candle SN with more precise data points and the standard chronometer $H(z)$ with more direct relations with the cosmological parameters of interest. Moreover, our results displayed in Fig 1 suggest that the principal axes of confidence regions obtained with QSO, SN and $H(z)$ are inclined at higher angles, which indicates that bigger and more accurate sample of the quasar data can act as a complementary probe to test the properties of dark energy and break the degeneracy in the IDE model parameters. This tendency could also be perceived from the more stringent constraints obtained from the combination of those three probes.

In the first case of the γ_c IWCDM model, in order to illustrate the performance of the quasar

Table 1: Distance ratios from recent BAO measurements.

Survey	z	$D_V(z)/r_s(z_d)$	$D_M(z)/r_s(z_d)$	$D_H(z)/r_s(z_d)$	Reference
6dFGS	0.106	3.047 ± 0.137	–	–	Beutler et al. (2011)
SDSS-MGS	0.15	4.480 ± 0.168	–	–	Ross et al. (2015)
BOSS-LOWZ	0.32	8.594 ± 0.095	8.774 ± 0.142	25.89 ± 0.76	Anderson et al. (2014)
BOSS-CMASS	0.57	13.757 ± 0.142	14.745 ± 0.237	21.02 ± 0.52	Anderson et al. (2014)
SDSS DR12	2.33	–	37.77 ± 2.73	9.07 ± 0.31	Bautista et al. (2017)

Table 2: The marginalized 1σ errors of the parameters Ω_{b0} , Ω_{c0} , w , γ_i , and H_0 for different interacting dark energy scenarios, as well as $\chi^2/d.o.f$ and FoM , obtained from the combinations of the data sets C1 (CMB+BAO), C2 (QSO+CMB+BAO) and C3 (QSO+CMB+BAO+SN+ $H(z)$), respectively. Corresponding results for the Λ CDM and WCDM models are also added for comparison.

Λ CDM	Ω_{b0}	Ω_{c0}	w	γ	H_0	$\chi^2/d.o.f$	FoM
C1	$0.0501^{+0.0011}_{-0.0010}$	$0.277^{+0.011}_{-0.011}$	-1	0	$66.48^{+0.81}_{-0.81}$	10.35/10	7.33×10^6
C2	$0.0500^{+0.0010}_{-0.0009}$	$0.276^{+0.010}_{-0.010}$	-1	0	$66.59^{+0.80}_{-0.80}$	364.55/130	7.37×10^6
C3	$0.0499^{+0.0009}_{-0.0008}$	$0.275^{+0.008}_{-0.008}$	-1	0	$66.66^{+0.79}_{-0.78}$	925.36/740	7.96×10^6
γ_c IACDM	Ω_{b0}	Ω_{c0}	w	γ_c	H_0	$\chi^2/d.o.f$	FoM
C1	$0.0487^{+0.0018}_{-0.0015}$	$0.277^{+0.009}_{-0.009}$	-1	$-0.0025^{+0.0027}_{-0.0022}$	$67.75^{+1.25}_{-1.50}$	8.95/9	2.95×10^9
C2	$0.0483^{+0.0015}_{-0.0013}$	$0.276^{+0.009}_{-0.009}$	-1	$-0.0029^{+0.0021}_{-0.0018}$	$68.04^{+1.01}_{-1.23}$	361.19/129	4.73×10^9
C3	$0.0485^{+0.0014}_{-0.0012}$	$0.276^{+0.009}_{-0.010}$	-1	$-0.0026^{+0.0018}_{-0.0018}$	$67.88^{+0.92}_{-1.03}$	921.38/739	5.51×10^9
γ_d IACDM	Ω_{b0}	Ω_{c0}	w	γ_d	H_0	$\chi^2/d.o.f$	FoM
C1	$0.0504^{+0.0011}_{-0.0011}$	$0.276^{+0.010}_{-0.013}$	-1	$-0.0052^{+0.0077}_{-0.0083}$	$66.45^{+1.04}_{-0.71}$	9.16/9	1.44×10^9
C2	$0.0504^{+0.0010}_{-0.0010}$	$0.275^{+0.010}_{-0.010}$	-1	$-0.0052^{+0.0077}_{-0.0083}$	$66.53^{+0.81}_{-0.70}$	363.24/129	1.59×10^9
C3	$0.0503^{+0.0010}_{-0.0010}$	$0.274^{+0.009}_{-0.010}$	-1	$-0.0057^{+0.0077}_{-0.0082}$	$66.64^{+0.77}_{-0.70}$	924.07/739	1.64×10^9
w CDM	Ω_{b0}	Ω_{c0}	w	γ	H_0	$\chi^2/d.o.f$	FoM
C1	$0.0517^{+0.0035}_{-0.0024}$	$0.282^{+0.013}_{-0.010}$	$-0.94^{+0.10}_{-0.08}$	0	$65.61^{+1.28}_{-2.03}$	8.86/9	1.01×10^8
C2	$0.0515^{+0.0034}_{-0.0024}$	$0.281^{+0.012}_{-0.011}$	$-0.95^{+0.10}_{-0.07}$	0	$65.83^{+1.24}_{-2.01}$	363.29/129	1.05×10^8
C3	$0.0500^{+0.0029}_{-0.0020}$	$0.275^{+0.012}_{-0.010}$	$-0.99^{+0.09}_{-0.07}$	0	$66.64^{+1.23}_{-1.73}$	925.13/739	1.31×10^8
γ_c IWCDM	Ω_{b0}	Ω_{c0}	w	γ_c	H_0	$\chi^2/d.o.f$	FoM
C1	$0.0509^{+0.0069}_{-0.0066}$	$0.282^{+0.015}_{-0.016}$	$-0.95^{+0.14}_{-0.15}$	$-0.0008^{+0.0044}_{-0.0042}$	$65.96^{+4.69}_{-4.06}$	8.76/8	1.26×10^{10}
C2	$0.0483^{+0.0045}_{-0.0040}$	$0.277^{+0.012}_{-0.012}$	$-1.00^{+0.11}_{-0.11}$	$-0.0026^{+0.0026}_{-0.0023}$	$67.96^{+2.79}_{-2.89}$	361.19/128	4.50×10^{10}
C3	$0.0476^{+0.0029}_{-0.0026}$	$0.274^{+0.010}_{-0.010}$	$-1.03^{+0.08}_{-0.07}$	$-0.0029^{+0.0019}_{-0.0017}$	$68.62^{+1.71}_{-2.05}$	921.16/738	8.88×10^{10}
γ_d IWCDM	Ω_{b0}	Ω_{c0}	w	γ_d	H_0	$\chi^2/d.o.f$	FoM
C1	$0.0514^{+0.0050}_{-0.0041}$	$0.281^{+0.020}_{-0.017}$	$-0.96^{+0.18}_{-0.14}$	$-0.0022^{+0.0135}_{-0.0120}$	$65.83^{+2.46}_{-3.14}$	8.85/8	6.26×10^9
C2	$0.0510^{+0.0041}_{-0.0040}$	$0.278^{+0.017}_{-0.016}$	$-0.97^{+0.14}_{-0.15}$	$-0.0042^{+0.0127}_{-0.0109}$	$66.06^{+2.60}_{-2.58}$	363.13/128	8.08×10^9
C3	$0.0499^{+0.0028}_{-0.0030}$	$0.273^{+0.013}_{-0.014}$	$-1.02^{+0.11}_{-0.11}$	$-0.0070^{+0.0109}_{-0.0097}$	$66.79^{+2.01}_{-1.73}$	923.94/738	1.64×10^{10}

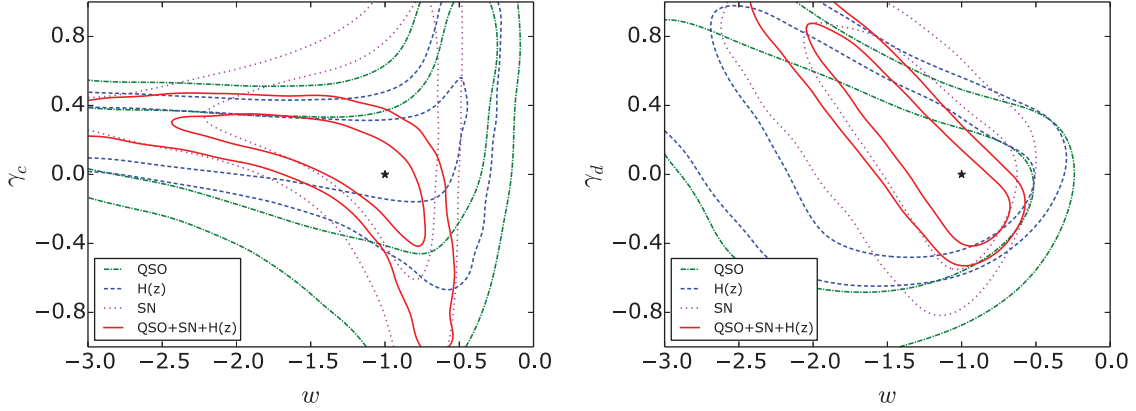


Fig. 1.— 1σ and 2σ confidence regions in the (w, γ_i) for the γ_c IWCMDM model (left panel) and γ_d IWCMDM model (right panel), which are derived from three different types of standard probes (QSO, SN and $H(z)$).

data, we choose three combinations of data sets and show the 1-D probability distribution of each parameter (Ω_{b0} , Ω_{c0} , w , γ_c , and H_0) and 2-D plots for the combinations of these parameters in Fig. 2. The corresponding marginal 1σ uncertainties can also be seen in Table. 2. Fitting results from the joint angular diameter distance data of QSO+CMB+BAO give the best-fit value for the interaction parameter and cosmic equation of state: $\gamma_c = -0.0026^{+0.0026}_{-0.0023}$, $w = -1.00^{+0.11}_{-0.11}$. For comparison, statistical standard rulers (CMB+BAO) without quasars are also given in Fig. 2, with the best-fit of the two parameters: $\gamma_c = -0.0008^{+0.0044}_{-0.0042}$, $w = -0.95^{+0.14}_{-0.15}$. Through the comparison of these plots, one can clearly see that the currently compiled quasar data may improve the constraints on model parameters significantly. The contours constrained with the total combination of three types of standard probes (QSO+CMB+BAO+SN+ $H(z)$) are also presented in Fig. 2, with the best-fit parameters: $\gamma_c = -0.0029^{+0.0019}_{-0.0017}$, $w = -1.03^{+0.08}_{-0.07}$. From the above results, the parameter γ_c capturing the interaction between DE and DM seems to be vanishing or slightly smaller than 0, which has been noticed by using the 182 Gold SNIa together with CMB and large-scale structure for the interacting holographic DE model (Feng et al. 2007) and by using the revised Hubble parameter data together with CMB and BAO (Cao et al. 2013). The sample of 59 high redshift calibrated Gamma-Ray Burst (GRB) data, whose redshift region is more comparable to our quasar data, combined with BAO observation from SDSS and CMB from the 7-Year Wilkinson Microwave Anisotropy Probe (WMAP7) also support this result (Pan et al. 2012). In general, for the two standard ruler data sets, at the 1σ confidence region, the energy is seen transferred from dark matter to dark energy, and the concordance model cannot be excluded. However, for the total combination of three types of standard probes, the concordance Λ CDM ($\gamma_c = 0, w = -1$) is almost excluded at 2σ error region. Similar conclusions could also be obtained from the γ_c IACDM model with $w = -1$, with the estimation of these cosmic parameters briefly summarized in Table. 2.

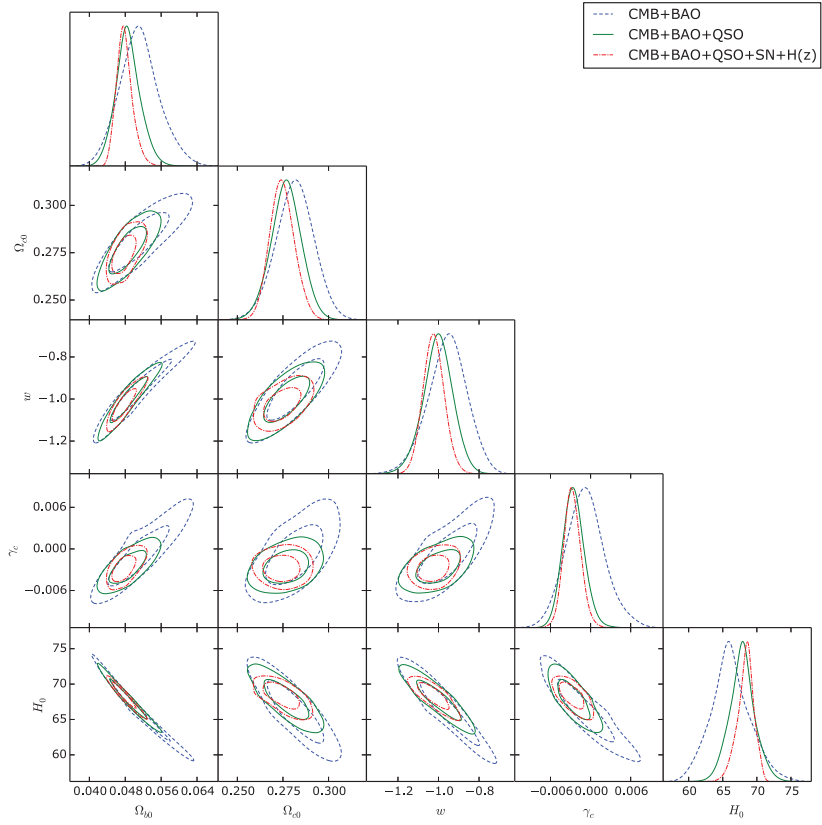


Fig. 2.— The 2-D regions and 1-D marginalized distribution with the 1- σ and 2- σ contours of the γ_c IWCDM model parameters (Ω_{b0} , Ω_{c0} , w , γ_c , and H_0) with the combined standard rulers (QSO+CMB+BAO), statistical standard rulers (CMB+BAO), and three types of standard probes.

Working on the γ_d IWCDM model when the interaction is proportional to the dark energy density ρ_X , we find that the best fits happen at $\gamma_d = -0.0022_{-0.0120}^{+0.0135}$ and $\gamma_d = -0.0042_{-0.0109}^{+0.0127}$ with statistical and combined standard ruler data, respectively. With the three types of standard probes (QSO+CMB+BAO+SN+ $H(z)$), we get the marginalized 1σ constraints of the parameters: $\Omega_{b0} = 0.0499_{-0.0030}^{+0.0028}$, $\Omega_{c0} = 0.273_{-0.014}^{+0.013}$, $w = -1.02_{-0.11}^{+0.11}$, $\gamma_d = -0.0070_{-0.0097}^{+0.0109}$, $H_0 = 66.79_{-1.73}^{+2.01}$ km/s/Mpc. Obviously, from the fitting results shown in Fig. 3 and Table. 2, Λ CDM ($\gamma_d = 0, w = -1$) is still included within 1σ error region and the joint analysis provides a small negative coupling which agrees with the results by using the Gold SNIa together with CMB and large-scale structure for other interacting DE models describing the interaction in proportional to the DM energy density (Guo et al. 2007). In addition, the constraining results in this work with the joint observational data including quasars are more stringent than previous results for constraining γ_d IDE model parameters with other combined observations arising from the 182 Gold SNe Ia samples, the shift parameter of CMB given by the WMAP3 observations, the BAO measurement from the Sloan Digital Sky Survey, the age estimates of 35 galaxies (Feng et al. 2008) and the 13 $H(z)$ measurements from the differential ages of red-envelope galaxies as well as the BAO peaks (Cao et al. 2013). Similar conclusions could also be obtained from the γ_d I Λ CDM model with $w = -1$, with the estimation of these cosmic parameters briefly summarized in Table. 2.

Now it is worthwhile to make some comments on the results obtained above. Firstly, concerning the interaction term between dark energy and dark matter, the statistical analysis based on three types of standard probes demonstrates that the parameter describing the interaction between DE and DM seems to be vanishing or slightly smaller than zero. At the 68.3% confidence level, the energy is seen transferred from dark matter to dark energy, which implies that the IDE models can not alleviate the coincidence problem or even make it more sever. This conclusion is consistent with the previous results for constraining IDE model parameters with other combined observations. Secondly, the estimated values of the Hubble constant are in agreement with the standard ones reported by *Planck* (Planck Collaboration XIII 2016). However, we still find strong degeneracies between γ_i and H_0 , i.e., a negative value of interaction term will lead to a larger value of the Hubble constant, which may alleviate the tension of H_0 between the recent *Planck* and *HST* measurements.

Finally, we would like to discuss statistically the performance of our data sets and perform model selection. On the one hand, in order to quantify the constraining power of the quasar data on cosmological model parameters, we calculate the Figure of Merit (FoM) for the IDE models with different data combinations. Based on the the previous definition proposed by the Dark Energy Task Force (DETF) for the CPL parametrization (Albrecht et al. 2006), a more general expression

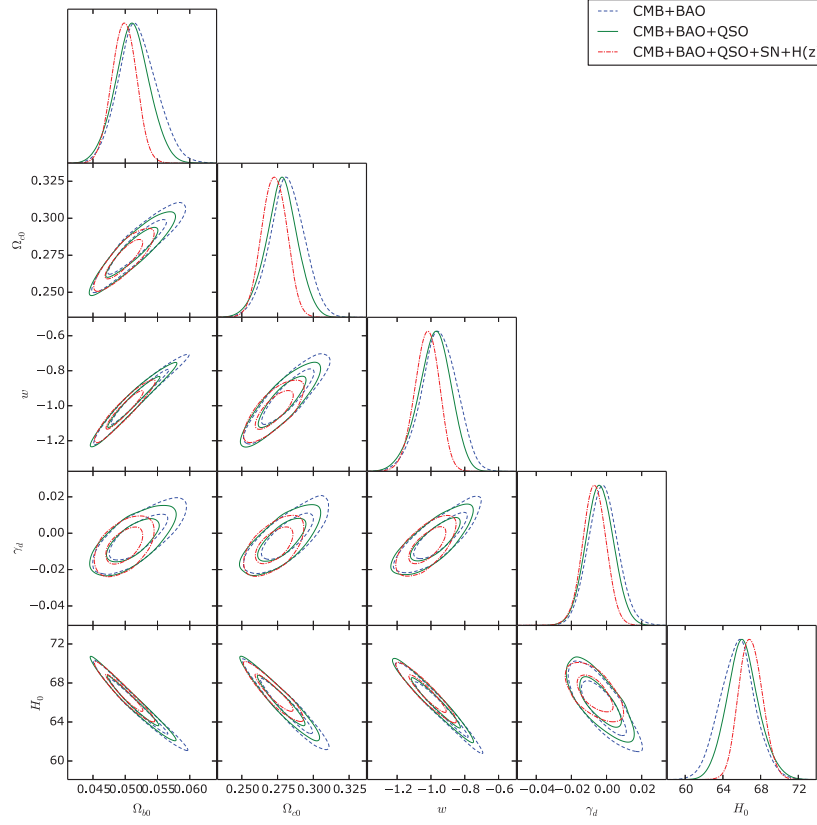


Fig. 3.— The same as Fig. 2, but for the $\gamma_d I\Lambda CDM$ model.

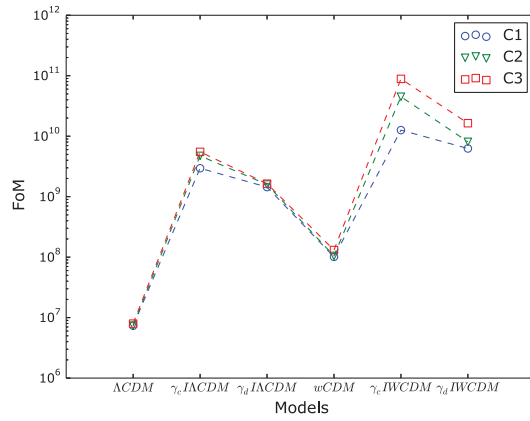


Fig. 4.— The FoM value for each cosmological model calculated from different data combinations: C1 (CMB+BAO), C2 (QSO+CMB+BAO) and C3 (QSO+CMB+BAO+SN+ $H(z)$).

can be rewritten as (Wang 2008)

$$FoM = (\det Cov(\mathbf{p}))^{-1/2} \quad (21)$$

where $Cov(\mathbf{p})$ is the covariance matrix of relevant cosmological parameters \mathbf{p} . Higher value of the FoM is corresponds to tighter model constraint. From the results shown in Fig. 4 and Table 2, one can clearly see that the inclusion of the QSO sample will generate more stringent constraints on the interacting dark energy models, especially for the γ_c WIDE model. This can be understood in terms of a higher redshift range covered by QSOs in comparison to other cosmological probes. On the other hand, in the face of so many competing interacting dark energy scenarios, it is important to find an effective way to decide which one is most favored by the data. Following the analysis of Biesiada (2009) and Cao & Zhu (2011), model comparison statistics including the Akaike Information Criterion (AIC) (Akaike 1974) and the Bayesian Information Criterion (BIC) (Schwarz 1978) will be used for this purpose. The expression of the two main information criteria can be written as

$$AIC = -2\ln\mathcal{L}_{max} + 2k = \chi_{min}^2 + 2k \quad (22)$$

and

$$BIC = -2\ln\mathcal{L}_{max} + 2\ln N = \chi_{min}^2 + k\ln N \quad (23)$$

where $\mathcal{L}_{max} = \exp(-\chi_{min}^2/2)$ is the maximum likelihood value, k is the number of free parameters in the model and N is the total number of data points used in the statistical analysis.

Table 3 lists the AIC and BIC difference of each model. One can see that the two criteria lead to different conclusions, concerning the ranking of competing dark energy models. More specifically, according to the AIC, the γ_c IACDM performs the best, while the γ_d IWCDM model gets the smallest support from the current observations. On the contrary, the BIC criterion gives a different ranking: the cosmological constant model is still the best cosmological model. Then comes the sequence: XCDM, γ_c IACDM, and γ_d IACDM with one more free parameter, while γ_c IWCDM and γ_d IWCDM are clearly disfavored by the data. Therefore, our findings indicate that interacting dark energy models with more free parameters are substantially penalized by the BIC criterion, which agrees very well with the previous results derived from other cosmological probes including strong lensing systems (Biesiada et al. 2010; Cao & Zhu 2011; Li et al. 2016).

5. Conclusions

In this paper, using the newly released data, derived from the very-long-baseline interferometry (VLBI) observations, comprising redshifts and angular sizes of compact structure in radio quasars, we have examined several popular phenomenological interaction models for dark energy and dark matter. Such models were proposed to alleviate the coincidence problem of the concordance Λ CDM model as well the tension between H_0 derived from the recent *Planck* and *HST* measurements. The sub-sample of 120 intermediate-luminosity quasars in the redshift range of $0.46 < z < 2.8$, which

Table 3: Summary of the information criteria for different interacting dark energy scenarios, obtained from the combinations of the data sets: C1 (CMB+BAO), C2 (QSO+CMB+BAO) and C3 (QSO+CMB+BAO+SN+ $H(z)$). Corresponding results for the Λ CDM and w CDM models are also added for comparison.

Data	Model	k	AIC	ΔAIC	BIC	ΔBIC
C1 ($N = 13$)	Λ CDM	3	16.35	0	18.04	0
	$\gamma_c I \Lambda$ CDM	4	16.95	0.60	19.21	1.17
	$\gamma_d I \Lambda$ CDM	4	17.16	0.81	19.42	1.38
	w CDM	4	16.86	0.51	19.12	1.08
	$\gamma_c I w$ CDM	5	18.76	2.41	21.58	3.54
	$\gamma_d I w$ CDM	5	18.85	2.50	21.67	3.63
C2 ($N = 133$)	Λ CDM	3	370.55	1.36	379.22	0
	$\gamma_c I \Lambda$ CDM	4	369.19	0	380.75	1.53
	$\gamma_d I \Lambda$ CDM	4	371.24	2.05	382.80	3.58
	w CDM	4	371.29	2.10	382.85	3.63
	$\gamma_c I w$ CDM	5	371.19	2.00	385.64	6.42
	$\gamma_d I w$ CDM	5	373.13	3.94	387.58	8.36
C3 ($N = 743$)	Λ CDM	3	931.36	1.98	945.19	0
	$\gamma_c I \Lambda$ CDM	4	929.38	0	947.82	2.63
	$\gamma_d I \Lambda$ CDM	4	932.07	2.15	950.51	5.32
	w CDM	4	933.13	3.75	951.57	6.38
	$\gamma_c I w$ CDM	5	931.16	1.78	954.21	9.02
	$\gamma_d I w$ CDM	5	933.94	4.56	956.99	11.80

was extracted from 613 milliarcsecond ultra-compact radio sources observed by a 2.29 GHz VLBI all-sky survey, can be used as cosmological standard rulers with the linear sizes calibrated by a cosmological-model-independent method, $l_m = 11.03 \pm 0.25$ pc. Compared with the SN Ia standard candles ($z \sim 1.4$) extensively used in the cosmological study, the advantage of this data set is that quasars are observed at much higher redshifts ($z \sim 3.0$), which motivate us to investigate the possible interaction between dark energy and dark matter at higher redshifts. To reduce the uncertainty and put tighter constraints on the coupling parameters, we added, in our discussion, the CMB results from the *Planck* as well as the BAO measurements both from the low- z galaxy and higher- z Lyman- α Forest (Ly α F) data. We expect that sensitivities of measurements of different observables can give complementary results on the coupling between dark sectors. Moreover, in order to quantify the constraining power of the current quasar data on the model parameters and the ranking of competing dark energy models, we assessed the FoM and performed model comparison using information-theoretical techniques (AIC and BIC criteria). Here we summarize our main conclusions in more detail:

- The quasar data could provide constraints competitive to the other two types of standard probes, i.e., the SNIa as standard candles with more precise data points and cosmic chronometers providing $H(z)$ which are more directly related to the cosmological model parameters of interest. Moreover, our results showed that the principal axes of confidence regions obtained with QSO, SN and $H(z)$ are inclined at higher angles to each other, which indicates that more and precise quasar data can act as a complementary probe to test the properties of dark en-

ergy and break the degeneracy in the IDE model parameters. This conclusion is strengthened by the statistical results from the Figure of Merit, which supports the claim that inclusion of the QSO sample covering higher redshift range, leads to more stringent constraints on the interacting dark energy models (especially for the γ_c WIDE model).

- Concerning the interaction term between dark energy and dark matter, statistical analysis from the three types of standard probes, suggests that it is vanishing or slightly smaller than zero. At the 68.3% confidence level, the energy is seen transferred from dark matter to dark energy, which implies that those IDE models can not alleviate the coincidence problem or make it even more sever. This conclusion is consistent with the previous results concerning IDE model parameters obtained on other combined observations.
- The estimated values of the Hubble constant are in agreement with the standard ones reported by *Planck* (Planck Collaboration XIII 2016). However, strong degeneracies between γ_i and H_0 implying that negative value of the interaction term will lead to a larger value of the Hubble constant, may alleviate the tension between the recent *Planck* and *HST* measurements of H_0 .
- The AIC and BIC have provided quite different conclusions, concerning the ranking of competing dark energy models. More specifically, according to the AIC, the γ_c IACDM performs the best, while the γ_d IWCDM model gets the smallest support from the current observations. On the contrary, the BIC criterion gives a different ranking: the cosmological constant model is still the best cosmological model followed by the XCDM, γ_c IACDM, and γ_d IACDM, while γ_c IWCDM and γ_d IWCDM are clearly disfavored by the data. Therefore, our findings indicate that interacting dark energy models with more free parameters are substantially penalized by the BIC criterion, which agrees very well with the previous results derived from other cosmological probes.

6. Acknowledgments

This work was supported by the Ministry of Science and Technology National Basic Science Program (Project 973) under Grants No. 2014CB845806, the Strategic Priority Research Program “The Emergence of Cosmological Structure” of the Chinese Academy of Sciences (No. XDB09000000), the National Natural Science Foundation of China under Grants Nos. 11503001, 11373014 and 11073005, the Fundamental Research Funds for the Central Universities and Scientific Research Foundation of Beijing Normal University, China Postdoctoral Science Foundation under grant No. 2015T80052, and the Opening Project of Key Laboratory of Computational Astrophysics, National Astronomical Observatories, Chinese Academy of Sciences. X.Z. is supported by the China Scholarship Council. M.B. gratefully acknowledges support and hospitality of the Beijing Normal University.

REFERENCES

- Ade, P. A. R., et al. [Planck Collaboration] 2016, *A&A*, 594, A13
- Ade, P. A. R., et al. [Planck Collaboration] 2016, *A&A*, 594, A14
- Akaike, H. 1974, *IEEE Transactions on Automatic Control*, 716, 72, 3
- Albrecht, A., Bernstein, G., Cahn, R., et al. 2006, Report of the Dark Energy Task Force [arXiv:0609591]
- Amendola, L. 2000, *PRD*, 62, 043511
- Anderson, L., Aubourg, E., Bailey, S., et al., 2014, *MNRAS*, 441, 24
- Bautista, J. E., Busca, N. G., Guy, J., et al., 2017, *A&A*, in press [arXiv:1702.00176]
- Beutler, F., Blake, C., Colless, M., et al., 2011, *MNRAS*, 416, 3017 [arXiv:1106.3366]
- Biesiada, M., 2007, *JCAP*, 02, 003
- Biesiada, M., Piórkowska, A., & Malec, B. 2010, *MNRAS*, 406, 1055
- Bond, J. R., Efstathiou, G., & Tegmark, M., 1997, *MNRAS*, 291, L33
- Cao, S., Biesiada, M., Jackson, J., et al. 2017, *JCAP*, 02, 12
- Cao, S., Chen, Y., Zhang, J., & Ma, Y. B. 2015, *IJTP*, 54, 1492
- Cao, S., Liang, N., & Zhu, Z.-H. 2011, *MNRAS*, 416, 1099
- Cao, S., & Liang, N. 2013, *IJMPD*, 22, 1350082
- Cao, S., & Zhu, Z.-H. 2011, *PRD*, 84, 023005
- Cao, S., Zheng, X. G., Biesiada, M., et al. 2017, *A&A*, in press
- Costa, A. A., Xu, X. D., Wang, B., Abdalla, E., 2017, *JCAP*, 01, 028
- Dalal, N., Abazajian, K., Jenkins, E., et al. 2001, *PRL*, 87, 141302
- Ding, X. H., Biesiada, M., Cao, S., Li, Z. X., & Zhu, Z. H., 2015, *ApJ*, 803, L22
- Eisenstein, D. J., & Hu, W., 1998, *ApJ*, 496, 605
- Eisenstein, D. J., Zehavi, I., Hogg, D. W., et al. 2005, *ApJ*, 633, 560
- Feng, C., Wang, B., Gong, Y. G., & Su, R. K. 2007, *JCAP*, 09, 005
- Feng, C., Wang, B., Abdalla, E., & Su, R. 2008, *PLB*, 665, 118

- Guo, Z. K., Ohta, N., & Tsujikawa, S. 2007, PRD, 76, 023508
- Gurvits, L. 1994, ApJ, 425, 442
- Hu, W., & Sugiyama, N. 1996, ApJ, 471, 542
- Komatsu, E., et al. [WMAP Collaboration], 2009, AJS, 180, 330
- Komatsu, E., Smith, K. M., & Dunkley, J. et al. 2011, ApJS, 192, 18
- Lewis, A., & Bridle, S. 2002, PRD, 66, 103
- Li, X. L., Cao, S., Zheng, X. G., Li, S., & Biesiada, M. 2016, RAA, 16, 84
- Li, Y. H., Zhang, J. F., & Zhang, X. 2016, PRD, 93, 023002
- Olivares, G., Atrio-Barandela, F., & Pavon, D. 2006, PRD, 74
- Pan, Y., Cao, S., Gong, Y.-G., Liao, K., & Zhu, Z.-H. 2013, PLB, 718, 699
- Perlmutter, S., Aldering, G., Goldhaber, G., et al. 1999, ApJ, 517, 565
- Riess, A. G., Filippenko, A. V., Challis, P., et al. 1998, AJ, 116, 1009
- Riess, A. G., Macri, L. M., Hoffmann, S. L., et al. 2016, ApJ, 826, 56 [arXiv:1604.01424]
- Ross, A. J., Samushia, L., Howlett, C., et al. 2015, MNRAS, 449, 835
- Sahni, V., Shafieloo, A., & Starobinsky, A. A. 2014, ApJ, 793, L40
- Schwarz, G. 1978, Annals of Statistics, 15, 18
- Suzuki, N., Rubin, D., Lidman, C., et al. 2012, ApJ, 746, 85
- Wang, B., Abdalla, E., Atrio-Barandela, F., & Pavon, D. 2016, ROPP, 79, 096901 [arXiv:1603.08299]
- Wang, Y. 2008, PRD, 77, 123525 [arXiv:0803.4295]
- Will, C. M. 2001, Living Rev. Rel. 4, 4
- Xia, D. M., & Wai, S. 2016, MNRAS, 463, 952
- Zheng, X. G., Ding, X. H., Biesiada, M., et al. 2016, ApJ, 825, 17